materials

MDPI

Review

Review on Multi-Field Coupled Behavior of Large Precast Box Girders at Early Age: From Multi-Physics Modeling to Data-Driven Intelligent Prediction

Meng Zhou [1], Yuliang Cai [1,*], Huan Zhang [2] and Xiao Tan [3,*]

[1] Zhejiang Key Laboratory of Intelligent Construction and Operation & Maintenance for Deep-Sea Foundations, Ningbo University of Technology, Ningbo 315211, China
[2] Ningbo High Grade Highway Construction and Management Center, Ningbo 315199, China
[3] College of Water Conservancy and Hydropower Engineering, Hohai University, Nanjing 210024, China
* Correspondence: caiyuliang@nbut.edu.cn (Y.C.); xiaotan@hhu.edu.cn (X.T.)

Abstract

To improve the crack prevention and long-term service performance of large precast full-span concrete box girders at early age, this study systematically reviews the research progress on temperature fields, humidity fields, stress fields, and cracking risk assessment of large precast box girders, focusing on the key thermo-hydro-mechanical problems under the coupled effects of hydration heat, humidity evolution, shrinkage deformation, and creep. The applications of artificial intelligence and machine learning methods in early-age field prediction, thermal parameter inversion, and intelligent control of cracking risk are also reviewed and discussed. The main findings are as follows: hydration heat is the primary source of internal temperature rise in large precast box girders, and the hydration reaction rate is significantly affected by temperature; however, existing hydration heat models still inadequately account for temperature dependency and the time-varying characteristics of thermal parameters. Influenced by self-desiccation, moisture conduction and diffusion, and internal/external formwork constraints, significant humidity gradients readily develop within box girders. Humidity evolution and the associated shrinkage deformation exert important effects on early-age stress and crack development, yet existing studies still devote relatively insufficient attention to humidity fields and humidity-induced stresses. Regarding multi-field coupling, significant synergistic interactions exist among temperature, humidity, shrinkage, creep, and the time-varying properties of materials, while existing numerical simulation methods still possess certain limitations. For early-age cracking of box girders, the comprehensive consideration of multi-field coupling effects and time-varying material characteristics remains to be strengthened. With the advancement of artificial intelligence technologies, data-driven models enable efficient prediction of early-age temperature and humidity fields, and physics-informed neural networks can accomplish thermal parameter inversion and field reconstruction from sparse and noisy monitoring data. Nevertheless, challenges persist in terms of limited sample availability, physical consistency, interpretability, and uncertainty quantification. Future research should further establish multi-scale, multi-field coupled analysis frameworks that integrate temperature, humidity, shrinkage, creep, and time-varying material characteristics, and combine artificial intelligence and machine learning methods to construct an intelligent prediction and active control system for early-age cracking risk based on the integration of physics-constrained and data-driven approaches.

Check for updates

Academic Editor: Piotr Smarzewski

Received: 4 September 2026
Revised: 25 November 2026
Accepted: 26 November 2026
Published: 29 November 2026

Copyright: © 2026 by the authors. Licensee MDPI, Basel, Switzerland. This article is an open access article distributed under the terms and conditions of the Creative Commons Attribution (CC BY) license.

Keywords: large precast box girder; early-age concrete; multiphysics coupling; cracking risk assessment; data-driven; physics-informed neural networks; machine learning

1. Introduction

With the gradual advancement of industrialization, precast construction methods have been widely applied in bridge engineering. Compared with traditional precast-assembled small box girders and T-beam bridges, large-scale full-span precast box girders possess significantly fewer joints. This effectively overcomes the inherent structural defects associated with conventional longitudinal and transverse segmental (or component) assembled structures. Furthermore, they facilitate routine internal inspections and maintenance within the box during the later operational phase. Consequently, they have been extensively utilized in the construction of highway and railway bridges in China [1].

For high-speed railway bridges in China, the mainstream recommended girder type is the 32-m prestressed concrete simply-supported box girder, which features a relatively simple structural form. In contrast, large-scale full-span precast box girders for highways often adopt a construction method involving a structural system conversion from simply-supported to continuous. Due to this, numerous prestressed anchor blocks are arranged inside the box girders, resulting in a relatively complex structural configuration. Furthermore, the greater the tonnage of the box girder, the more internal anchor block structures are required. The cross-section of large-scale precast box girders is typically characterized by thicker girder ends and a thinner middle section, presenting a significant difference in wall thickness between the end sections and the mid-span section.

Table 1 summarizes recent highway engineering projects utilizing large-scale full-span precast concrete box girders. In 2006, the Hangzhou Bay Bridge achieved the world's first onshore precasting and girder transportation on existing beams, as well as launching gantry erection of 50-m-span, 1430-ton large-scale full-span concrete box girders [2]. Furthermore, it successfully accomplished the offshore erection of 70-m-span, 2200-ton large-scale full-span precast box girders in the open sea. This successful precedent demonstrates that the adoption of on-girder transportation technology can effectively overcome the limitations associated with the land transportation of large-tonnage precast components. Provided that navigational conditions permit, the over-water transportation and installation of large precast components no longer present any technical barriers. Consequently, this has further promoted the application of large-scale full-span precast box girders in highway engineering.

However, due to the combined effects of various factors, including intense hydration reactions, external environmental conditions, and shrinkage deformations [3–5], large-scale precast box girders are highly susceptible to early-age cracking during the early precasting phase (from final setting to the onset of the mature stage). Such early-age cracks not only severely impair the durability of the components but also significantly shorten the service life of the structure [6]. Particularly in marine environments, these cracks further accelerate chloride ingress and subsequent corrosion, which not only drastically increases the costs of later-stage maintenance and repair, but may also trigger catastrophic consequences, resulting in severe social impacts and economic losses.

Therefore, this paper reviews the early-age cracking issues faced by large-scale full-span precast concrete box girders during the precasting phase, as well as the current research status under the influence of factors such as hydration heat, ambient environment, autogenous shrinkage, and drying shrinkage. Furthermore, in line with the development trend of intelligent construction and operation & maintenance for infrastructure, this study also reviews research progress and provides an outlook on the applications of artificial

intelligence and machine learning methods in early-age field prediction, parameter inversion, and intelligent control of cracking risk for concrete.

Table 1. Highway engineering projects utilizing large-scale full-span precast box girders.

Project Name	Country/Region	Span Length (m)	Weight per Span (t)	Year of Construction/Opening
Hangzhou Bay Bridge	China	50/70	1430/2200	2008
Jintang Bridge	China	60	1575	2009
Yuci Expressway	China	35	800	2015
Sanmen Bay Bridge	China	40	1260	2018
Kuwait Bay Bridge	Kuwait	60	1700	2019
Zhoudai Bridge	China	70	1800	2021
Xiangshan Bay Port Expressway	China	35	1050	2023
Phase I of Hangzhou–Ningbo Expressway Duplication Ningbo Section (Offshore Section)	China	40/50	1300/1800	2024

The review searched the Web of Science Core Collection, Scopus, Engineering Village, CNKI and other relevant academic databases. The search covered publications from 1980 to 2026. Representative search terms included 'large precast box girder', 'early-age temperature field', 'hydration heat', 'internal relative humidity', 'moisture diffusion', 'autogenous shrinkage', 'drying shrinkage', 'early-age creep', 'thermo-hygro-mechanical coupling', 'machine learning', and 'physics-informed neural networks'. After removing duplicate records and excluding irrelevant studies through title, abstract, and full-text screening, 104 publications were finally selected for this review.

Furthermore, it critically evaluates the applicability and limitations of existing numerical models, identifies the insufficient understanding of humidity-induced stresses and comprehensive thermo-hygro-mechanical coupling, and explores the potential integration of machine learning and physics-informed neural networks into early-age field prediction. This review aims to provide insights and references for researchers and practitioners, thereby facilitating the high-quality construction and long-service-life operation of large-scale full-span precast concrete box girder bridges.

2. Computational Model for Early-Age Temperature Field of Large Precast Box Girders

At early ages, due to the hydration reaction of concrete, a substantial amount of heat is generated and accumulates within the core of large-scale full-span precast box girders. Driven by this non-uniform temperature distribution, thermal stresses are induced within the girder body. Once these thermal stresses become excessive, they will lead to concrete cracking.

Compared with conventional mass concrete structures (such as dams, pile caps, and bridge piers), large-scale precast box girders exhibit more complex geometries and heat dissipation conditions [7,8]. Moreover, since high-performance concrete (HPC) is frequently employed in their construction, the temperature effects induced by hydration heat are even more critical and cannot be ignored. Excessive temperature gradients will generate severe thermal stresses, leading to early-age cracking in large-scale precast box girders [9,10] and consequently compromising the durability of the bridges. Therefore, early-age hydration heat effects exert a profound impact on the early-stage construction of large-scale precast box girders [11] and directly dictate the casting quality of the girders.

As the hydration reaction proceeds, not only does the early-age temperature field of large-scale full-span precast box girders undergo drastic variations [12], but the physical states and properties of the concrete also evolve simultaneously. Temperature not only alters the early-age hydration reaction rate of the concrete, but the early-age thermal parameters also vary in response to temperature fluctuations and the evolution of concrete properties.

Although existing studies have investigated the early-age hydration heat temperature fields of large concrete structures—such as segmental box girders [13,14], cast-in-place continuous girders [6,15], steel-concrete composite bridges [16], and Block 0 of large-span prestressed concrete rigid frame bridges [17,18]—there remains a scarcity of research focused on large-scale precast box girders. Moreover, these studies tend to overlook the influence of temperature on the hydration reaction and thermal parameters. Hui [19] investigated the early-age temperature field of Block 0 in a large-span bridge and utilized Midas FEA for modeling; however, the study did not account for the effect of temperature on the hydration reaction rate and treated the thermal parameters as constants. Both Yu [20] and Wang [21] studied the early-age hydration heat temperature fields of single-box three-cell cast-in-place concrete box girders and evaluated the impact of thermal stresses on early-age cracking. Similarly, they neglected the influence of early-age temperature on both the hydration reaction rate and thermal parameters. Zhang [7] and Wang [22] employed ANSYS and Midas FEA, respectively, to study the early-age temperature fields of Block 0 in large-span prestressed continuous rigid frame bridges. Yet, their literature did not mention the effect of temperature on the autogenous heat generation equation and assumed thermal parameters (thermal conductivity and specific heat) to be constants. In a study on the early-age temperature field of steel-concrete composite bridges, Zhang [23] considered the effect of initial temperature on the chemical reaction rate but ignored the temperature's influence on thermal conductivity and specific heat. Through temperature testing and numerical simulations on concrete segmental box girders in Northwest China, Han et al. [24] primarily investigated the early-age temperature fields and thermal stresses under special environmental conditions but similarly overlooked the effect of temperature on early-age thermal parameters.

As evidenced by the aforementioned literature, previous studies tend to ignore the accelerating effect of elevated temperatures on the hydration reaction. Calculations are often based merely on the elapsed time since casting, which leads to discrepancies between the computed temperature fields and actual conditions. Furthermore, existing research typically sets thermal parameters as constants—thereby failing to account for the evolution of early-age concrete properties and the temperature dependence of these parameters. This results in deviations between the simulated and actual temperature fields during the early age of concrete (particularly within the first 3 to 4 days).

Due to the intense early-age hydration reaction, uneven temperature distribution, and significant temperature fluctuations in large-scale precast box girders, internal temperatures alter the hydration process. Consequently, this induces spatio-temporal non-uniformity in the hydration reaction rate, thermal conductivity, and specific heat of the girders. Previous studies have demonstrated that the specific heat of concrete varies with temperature during the early-age hydration process [25,26]. Influenced by temperature, the early-age thermal conductivity of concrete also exhibits significant variations [27,28]. To accurately simulate the early-age temperature fields of large-scale precast box girders, it is imperative to rigorously account for parameter variations during the processes of autogenous heat generation, heat conduction, and heat exchange. Ignoring these variations in finite element calculations can lead to inaccurate results, thereby adversely affecting early-age crack prevention in actual engineering practice [29,30]. According to the findings of Cai et al. [30], when the thermal parameters are treated as constants, the peak temperature of the box

girder differs by 2–3 °C compared with the case where the thermal parameters vary with equivalent age. Adopting the equivalent-age approach, which comprehensively accounts for the effects of temperature on both the hydration process and thermal properties, is currently the mainstream research methodology. The precise simulation of temperature fields provides a theoretical basis for early-age temperature regulation and curing process analysis of large-scale precast box girders; meanwhile, it serves as a crucial foundation for early-age thermal stress calculations. A comparison of representative numerical studies on the early-age temperature field of concrete structures is presented in Table 2.

Table 2. Comparison of representative numerical studies on early-age temperature fields of concrete structures.

Study	Structural Type	Numerical Software	Main Characteristics and Limitations
Zhang et al. [7]	Cast-in-place box girder zero block	ANSYS	Exponential hydration heat model; constant thermal conductivity and specific heat; convection boundary calibrated using measured environmental conditions; field temperature validation
Hui et al. [19]	Long-span variable-section box girder	MIDAS FEA	Thermal field analysis under construction conditions; temperature-dependent hydration and thermal parameter evolution were not fully considered
Yu et al. [20]	Three-cell concrete box girder model	DIANA	Large-scale sensor arrangement and consideration of solar radiation and wind effects; simplified model assumptions require further evaluation
Wang et al. [21]	Single-box three-cell girder model	DIANA	Model testing with embedded temperature and strain sensors; provides evidence of spatial temperature and strain variations
Zhang et al. [23]	Steel-concrete composite girder	ABAQUS 6.14 with USDFLD, UEXPAN and GETVRM	Initial-temperature influence on hydration reaction considered; temperature dependence of thermal conductivity and specific heat requires further consideration
Han et al. [24]	Concrete box girder in cold regions	ABAQUS 6.14 with USDFLD, UEXPAN and GETVRM	Investigates hydration temperature and early-age cracking under special environmental conditions
Cai et al. [30]	50 m precast concrete box girder	ABAQUS 2021 with UMATHT	Considers equivalent-age-dependent hydration and thermal properties; field tracking tests used for model validation

Currently, research on the early-age temperature fields of box girder structures primarily utilizes numerical simulations and experimental testing to investigate the time-history evolution patterns of temperatures and thermal stresses. However, there is relatively little research analyzing the specific factors influencing these early-age temperature fields. Moreover, in previous comparative analyses, the early-age thermal parameters of concrete are typically treated as constants. For instance, Zeng [31] conducted a parametric analysis on the curing of Block 0 in a concrete continuous rigid frame bridge. In their comparative analysis, the heat dissipation coefficient, thermal conductivity, and specific heat were all set as constants, without considering their variations with time and temperature, which ultimately led to discrepancies between the calculated results and the actual conditions.

3. Computational Model for Early-Age Humidity Field of Large Precast Box Girders

Moisture diffusion within the concrete of large-scale precast box girders leads to moisture loss in drying environments. This generates moisture gradients and induces moisture-induced stresses, which promote concrete surface cracking, especially the formation of early-age cracks.

Currently, insufficient attention is paid to drying shrinkage cracks in large-scale precast box girders caused by inadequate early-age curing. Previous studies have primarily focused on thermal cracks, and there are no reported studies regarding the early-age moisture fields and moisture-induced stresses in large-scale precast box girders; thus, further research is warranted. As a widely used porous composite material, the moisture diffusion properties of concrete significantly affect its various deterioration processes. Meanwhile, the moisture within concrete serves as a carrier for various aggressive agents. Therefore, an in-depth investigation into the moisture migration and diffusion mechanisms in large-scale precast box girders, along with the establishment of appropriate computational models and the formulation of mature control strategies, is of great significance for enhancing the durability of these girders.

In previous moisture field studies, researchers merely focused on small-scale ordinary concrete components. They conducted experimental moisture field tests by drilling holes and embedding humidity sensors [32–35], as shown in Figure 1. This method was used to analyze the distribution patterns and variation characteristics of concrete moisture fields; however, these studies generally did not consider the early-age autogenous shrinkage of concrete.

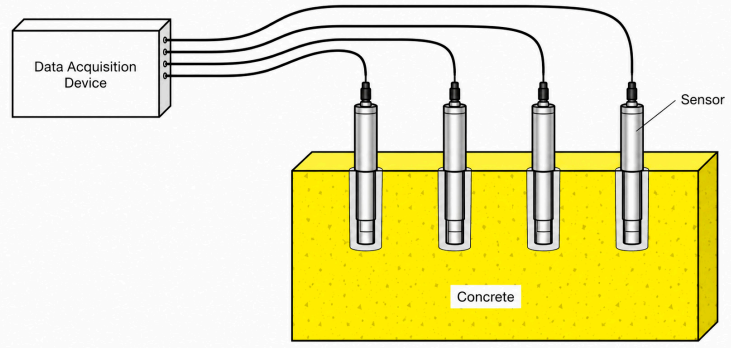


Figure 1. Traditional humidity field testing method.

Since the 21st century, with the widespread application of high-performance concrete in large-scale precast box girders, the issue of early-age autogenous shrinkage has become increasingly prominent [36]. The water–cement ratio of the concrete used in these large-scale precast box girders is typically around 0.3. Due to this low water–cement ratio, the early-age autogenous shrinkage effect is pronounced. According to the research by Tazawa and Miyazawa [37], when the water–binder ratio is less than 0.4, the autogenous shrinkage of concrete must be given due attention. At a water–binder ratio of 0.3, the autogenous shrinkage of silica fume-blended concrete is roughly equal to its drying shrinkage. When the water–binder ratio is less than 0.3, autogenous shrinkage becomes the dominant type of shrinkage in concrete. It is evident that the lower the water–binder ratio, the greater the proportion of autogenous shrinkage in the total shrinkage of concrete. Therefore, when calculating the early-age moisture fields of large-scale precast box girders, the influence of self-desiccation must be simultaneously considered [38].

In summary, the early-age moisture fields of large-scale precast box girders are primarily governed by the combined effects of self-desiccation, moisture conduction, and moisture

diffusion [39]. Accurate calculation of the moisture field is beneficial for analyzing concrete deformations induced by early-age drying shrinkage and autogenous shrinkage in box girders; moreover, it serves as a critical foundation for the analysis of moisture-induced stresses and comprehensive combined stresses.

Currently, moisture field testing is a vital means to control early-age shrinkage cracks. For large-scale full-size structures in actual engineering, the method of drilling holes to embed humidity sensors may adversely affect the structure's long-term service performance. Consequently, there are currently no reported experimental studies on the moisture fields of large-scale full-size structures in the literature; most studies are confined to laboratory tests on small-scale components [35,40]. The humidity sensors used in traditional concrete moisture field testing are predominantly air humidity sensors. These require drilling holes for embedment and sealing at the interface between the concrete surface and the sensor, thereby measuring the relative humidity of the air within the concrete pores to characterize the concrete's moisture status. Inadequate sealing at the contact area between the sensor and the concrete often leads to testing errors [41]. In the future, researchers could develop novel measurement methods and monitoring systems, including embedded moisture sensors and other indirect moisture measurement techniques, to enhance the accuracy of experimental data and the convenience of testing. A comparison of techniques for monitoring internal humidity in concrete structures is shown in Table 3.

Table 3. Comparison of Internal moisture monitoring technologies for concrete structures.

Technique	Measurement Principle	Advantages	Main Limitations	Suitability for Precast Girders
Drilled-hole RH probe	Measures RH in an equilibrated air cavity	Direct internal RH measurement; relatively mature method	Requires drilling and sealing; local disturbance; measurement delay	Suitable for laboratory validation and selected field locations
Embedded RH sensor	Measures RH using a sensor installed before casting	Continuous monitoring; no subsequent drilling; suitable for long-term measurements	Calibration drift; temperature sensitivity; installation and protection requirements	Particularly promising for full-scale monitoring

By adopting reasonable moisture testing methods, the internal moisture variations in concrete structures can be monitored in real-time to understand the real-time distribution of moisture fields. Based on on-site monitoring data, the early-age moisture fields of concrete box girders can also be evaluated, allowing for the timely implementation of corresponding control measures to prevent early-age drying shrinkage cracks.

4. Computational Model for Early-Age Stress Field of Large Precast Box Girders

During the early-age setting and hardening process, the concrete of large-scale precast box girders is subjected to the influences of hydration heat, ambient temperature and humidity, autogenous shrinkage, drying shrinkage, and creep. These factors collectively induce both elastic and inelastic deformations in the concrete. If these deformations are restrained by internal or external conditions, additional stresses will be generated within the concrete. Compared with elastic stresses, creep alters the magnitude of early-age autogenous stresses in concrete; meanwhile, creep is also influenced by the degree of hydration and temperature of the concrete [42]. Consequently, research on the early-age stresses of large-scale precast box girders is inherently highly complex. Previous studies on early-age cracking in box girders have often neglected early-age concrete shrinkage and creep effects, typically analyzing only elastic thermal stresses. To investigate the true early-age stress state of large-scale precast box girders and accurately analyze the causes

of early-age cracking, it is necessary not only to focus on the early-age temperature and moisture fields but also to clarify the relatively complex shrinkage deformations and creep effects at early ages.

4.1. Early-Age Shrinkage Deformations of Concrete

The total shrinkage deformation of concrete mainly comprises plastic shrinkage, autogenous shrinkage, drying shrinkage, and carbonation shrinkage. These shrinkage phenomena are inevitable during the hardening process, primarily caused by internal moisture loss and chemical reactions. Under restrained conditions, the stresses generated by shrinkage can lead to structural cracking. Therefore, the impact of shrinkage must be carefully considered during the calculation of early-age stress fields to ensure the reliability and authenticity of the computations. The primary types of concrete shrinkage deformations are as follows:

(1) Plastic Shrinkage

Plastic shrinkage refers to the volume change that occurs in freshly cast concrete prior to hardening [43]. It is primarily caused by early-age moisture evaporation or bleeding phenomena in the concrete [44]. Plastic shrinkage predominantly occurs between 3 and 12 h after initial setting and before final setting [45]. When the evaporation rate exceeds the rate of bleeding, the formation of capillary menisci and the resulting negative pore pressure may induce substantial surface contraction. In this review, attention is primarily focused on early-age stresses and cracking of concrete during the hardening stage.

(2) Autogenous Shrinkage

Autogenous shrinkage refers to the phenomenon where, during the hardening process, the autogenous hydration reaction consumes internal moisture, leading to a decrease in internal relative humidity and a subsequent reduction in the apparent volume (or length) of the concrete [46]. Chemical shrinkage refers to the phenomenon in which the absolute volume of hydration products is smaller than the total volume of the reactants during cement hydration. Before initial setting, autogenous shrinkage equals chemical shrinkage; after the initial structure has formed, autogenous shrinkage is less than chemical shrinkage, and chemical shrinkage equals the sum of autogenous shrinkage and the volume of pores formed. Autogenous shrinkage mainly occurs in the early stages following the formation of the initial concrete structure. With the widespread application of high-performance concrete, autogenous shrinkage has become one of the primary causes of early-age cracking [47]. Therefore, the effect of autogenous shrinkage must be considered in the early-age stress analysis of large-scale precast box girders.

(3) Drying Shrinkage

Drying shrinkage is the shrinkage phenomenon caused by the loss of internal moisture when concrete is exposed to a drying environment. Its mechanism involves the generation of calcium silicate hydrate (C-S-H) and the formation of numerous pores during cement hydration. Under external environmental actions, the liquid water in the concrete's micropores continuously evaporates, a process that propagates from the surface to the interior. The evaporation of liquid water in these capillary pores generates negative capillary pressure. The resulting liquid meniscus exerts tensile stresses on the pore walls (i.e., the C-S-H gel skeleton), causing the cement paste to shrink [48], as illustrated in Figure 2. When the shrinkage deformation of the concrete is restrained, the resulting excessive tensile stresses can cause the concrete surface to crack. This phenomenon is particularly pronounced in dry climates or well-ventilated environments [49]. Drying shrinkage is a primary cause of surface crack formation in

concrete. For mass concrete structures in particular, if early-age curing is neglected, cracking problems induced by drying shrinkage become even more severe [50]. Consequently, the effects of early-age drying shrinkage must also be considered in the early-age stress research of large-scale precast box girders.

(4) Carbonation Shrinkage

Carbonation shrinkage refers to the shrinkage phenomenon induced by the carbonate chemical reaction in concrete. When calcium hydroxide in the concrete reacts with carbon dioxide to form calcium carbonate, it is accompanied by volume shrinkage [51]. Carbonation shrinkage is a relatively slow process that typically only occurs after several years of concrete service [48]. For long-term operated concrete structures, carbonation shrinkage may lead to a degradation in structural stability and durability. However, in the context of early-age cracking research in large-scale precast box girders, carbonation shrinkage is generally negligible.

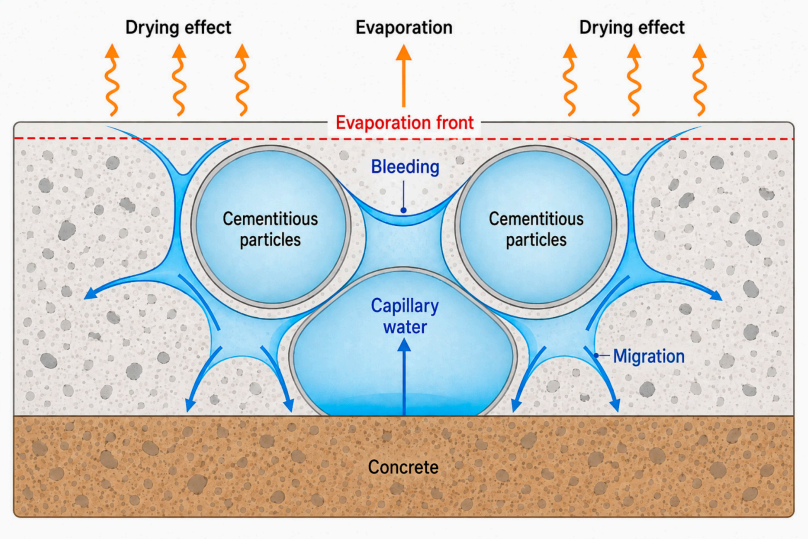


Figure 2. Schematic diagram of moisture transport in concrete.

Regarding concrete shrinkage deformation, the shrinkage models provided in design codes [52] are primarily applicable to concrete with strength grades ranging from C25 to C50 [53]. The shrinkage formulas in bridge design codes do not distinguish between autogenous shrinkage and drying shrinkage. Furthermore, the onset time of concrete shrinkage is conventionally assumed to be 3 to 7 days. Therefore, these code models may be inapplicable for calculating early-age shrinkage (from final setting to 100 h).

For concrete shrinkage, other models such as ACI 209, CEB-FIP 1990, and GL2000 are well-established predictive methods. However, their applicability during the first few days after concrete placement depends on the model formulation, the initial drying age, curing conditions, and the calibration of material parameters. Since the early-age shrinkage deformation of large-scale precast box girders is primarily governed by autogenous shrinkage and drying shrinkage, the controlling factors align with those considered in early-age moisture field research. Therefore, based on the analysis of early-age moisture fields, further research on the early-age shrinkage deformation and shrinkage-induced stresses of large-scale precast box girders can be systematically conducted.

4.2. Early-Age Creep Effects of Concrete

Early-age creep of concrete refers to an inelastic property that develops over time when the structure is subjected to sustained loads or stresses. There are various explanations for its underlying mechanisms [54,55].

Currently, the long-term creep models widely used worldwide include the CEB-FIP series, ACI series, GL2000, B3, AASHTO, and BS-5000 models, as well as Chinese domestic models such as JTG 3362-2018, TB 1002.3-2005, and the CABR-1986 model (China Academy of Building Research) [56]. These models are all constructed based on empirical or semi-empirical theoretical formulas. The establishment mechanisms vary among different models, and the selection of parameters has distinctive characteristics. To comprehensively consider the influences of various material parameters and environmental factors on creep, researchers have conducted statistical regression analyses based on extensive experimental data to determine empirical parameters for constructing prediction models.

However, in the first few days immediately after casting, the concrete has not fully solidified. Its shrinkage and creep behaviors are often influenced by multiple factors, such as temperature and humidity variations, as well as concrete mix proportions. These factors make it difficult to accurately predict and calculate concrete behavior. To avoid computational uncertainties and potential errors, concrete design codes generally do not account for the shrinkage and creep behaviors occurring in the first few days post-casting. Design codes [52,57] typically only provide calculation methods for concrete shrinkage and creep starting from 3 days of age.

An increasing number of studies [58,59] indicate that early-age creep effects in concrete are more pronounced than long-term ones. Rasmussen [60] adopted the Westman creep prediction model and used the relaxation coefficient method; the analysis revealed that creep caused a reduction in peak stress by approximately 60%. Furthermore, Zhang et al. [61,62] utilized the stress relaxation coefficient method to establish calculation methods for nonlinear thermal stresses and moisture shrinkage stresses considering creep effects. Their results showed that creep reduced the stresses by about 40%. Wei et al. [63], combining their analysis with the ABAQUS program and employing a creep function, found that creep reduced moisture warping and moisture-induced stresses by 36% and 45%, respectively. Hu et al. [64] analyzed the early-age behavior of concrete slab structures and demonstrated that creep reduced early-age warping by 82%. It can thus be concluded that the thermal and moisture stresses generated in early-age concrete under restrained conditions are significantly mitigated by concrete creep effects [65]. Consequently, thermal and moisture stress results calculated solely based on elastic theory are considerably higher than the actual stress values generated in engineering practice [66].

To more accurately describe and predict early-age creep behavior in concrete, researchers have conducted extensive work and proposed corresponding theories and models. These include the seepage theory, plastic flow theory, viscous flow theory, viscoelastic (anelastic) theory [67], micro-cracking theory [68], solidification theory [69,70], and microprestress-solidification (MPS) theory [71,72]. However, a unified consensus has yet to be reached.

For mass concrete and medium-volume reinforced concrete with low reinforcement ratios, creep deformation can generally be evaluated using linear creep theory [73]. Based on the form of the creep equations, they can be broadly classified into two categories. The first category treats the creep function as a function of the age at loading and the duration of loading, with its general expression shown in Equation (1):

$$J(t,\tau) = \frac{1}{E(\tau)}[1 + \varphi_0 f(\tau) g(t-\tau)] \quad (1)$$

In Equation (1), t is the curing age; τ is the loading age; $E(\tau)$ denotes the elastic modulus of concrete at the time of loading; φ_0 is the creep constant; $f(\tau)$ represents a function dependent on the age at loading; and $g(t-\tau)$ represents a function dependent on the duration of loading.

In another category of creep models, the recoverable delayed elastic deformation and the irrecoverable viscous flow deformation are incorporated. Its general expression is shown in Equation (2):

$$J(t,\tau) = \frac{1}{E(\tau)} + \varphi_1 f(t-\tau) + \varphi_2[g_2(t) - g_2(\tau)] \quad (2)$$

In Equation (2), t is the curing age; τ is the loading age; $E(\tau)$ denotes the elastic modulus of concrete at the time of loading; φ_1 and φ_2 denote the creep constants; $f(t-\tau)$ represents a function dependent on the duration of loading; and $g_2(t)$ and $g_2(\tau)$ represent functions of the curing age and the loading age, respectively.

In the field of concrete creep research, one model is often an evolution or modified version of another, with the primary differences lying in their accuracy, simplicity, and applicability. Professor Z. P. Bažant from Northwestern University proposed the Double Power Law (DPL) model specifically for early-age concrete. This model simulates early-age concrete creep based on the principle of linear superposition. Relevant studies have verified that this creep function can excellently simulate the creep characteristics of early-age concrete [40,74,75], as expressed in Equation (3):

$$J(t,\tau) = \frac{1}{E_0} + \frac{q}{E_0}\left(\alpha + \tau^{-d}\right)(t-\tau)^p \quad (3)$$

In Equation (3), t is the curing age, τ is the loading age, E_0 is the elastic modulus of concrete at loading, and $t-\tau$ is the load duration. α denotes the long-term creep model parameter; for short-term creep simulations, it can be assumed to be 0. The variables q, d, and p are material parameters. According to the literature [3,75], for early-age concrete research, the values of these material parameters are typically adopted as q = 0.6, d = 0.2, and p = 0.2, respectively. For different types of concrete, the model parameters need to be properly calibrated.

4.3. Early-Age Thermo-Hygro-Mechanical Coupling Effects in Large-Scale Precast Box Girders

Since variations in the early-age temperature and moisture fields of large-scale precast box girders occur continuously, the thermal deformations and hygral deformations generated by their coupling act directly on the concrete. Therefore, a comprehensive analysis of the time-dependent behavior of concrete under these coupling effects is crucial for analyzing early-age cracking [76,77]. Previous studies [78] typically analyzed only thermal stresses, often neglecting early-age concrete creep effects and the impact of moisture on early-age cracking. This omission makes it difficult to accurately identify the causes of cracking and propose effective countermeasures. The thermo-hydro-mechanical multi-field coupling mechanism of large precast box girders at early age is illustrated in Figure 3. The fully coupled mechanism and early-age shrinkage and creep still require further investigation.

Wang [79] investigated the early-age cracking issue in a prestressed cast-in-place continuous box girder and analyzed the impact of thermal stresses. However, the study did not consider early-age concrete shrinkage or creep effects, resulting in discrepancies between the analytical results and actual conditions. Consequently, accurate prevention and control measures for early-age cracks could not be effectively proposed. Yan et al. [80] conducted research on the causes and prevention measures of early-age cracks for a prestressed concrete cast-in-place continuous box girder. However, in their finite element analysis, the evolution of early-age mechanical properties of the concrete was ignored; both the elastic modulus and the coefficient of linear thermal expansion were assumed to be constant values. Furthermore,

early-age concrete shrinkage and creep effects were not considered, and the causes of early-age cracking were analyzed solely through elastic thermal stresses. This approach yielded results that deviated significantly from actual conditions. Liang et al. [81] carried out an analysis of the early-age temperature field and thermal stresses for Block 0 of a large-span bridge, but similarly failed to account for early-age concrete shrinkage and creep effects in their study.

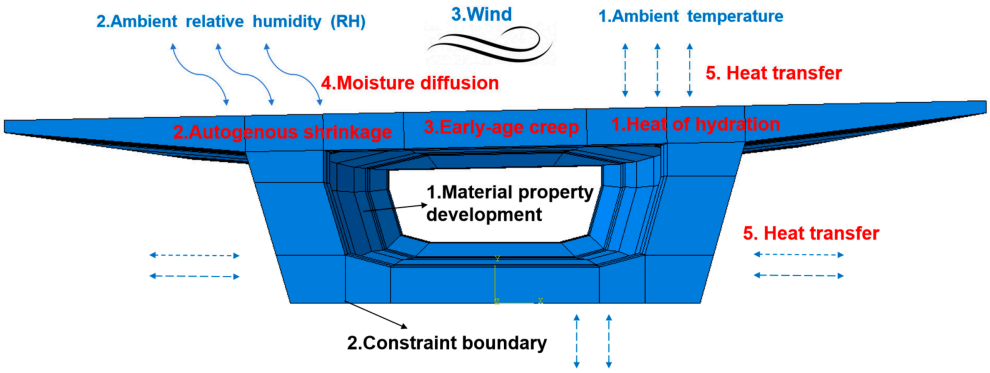


Figure 3. Schematic diagram of early-age thermo-hygro-mechanical multi-field coupling mechanism of large precast box girders.

In addition, employing numerical analysis methods, Srimook et al. [82] established an early-age thermo-mechanical coupling model to investigate the early-age cracking of massive reinforced concrete walls, quantitatively analyzing the causes of early-age cracks. However, their study did not consider the influence of early-age drying shrinkage on cracking. Qiao et al. [83] investigated the early-age cracking of steam-cured box girders by establishing a thermo-mechanical coupling model, analyzing the impact of relevant factors on early-age cracking. Yet, the absence of early-age concrete shrinkage and creep effects in their study led to certain deviations between the calculated results and reality. Furthermore, Li et al. [84] analyzed the causes of early-age cracking in the webs of Block 0 for a large-span bridge and concluded that shrinkage induced by moisture gradients was the primary cause of web cracking. This study was the first to highlight the importance of moisture-induced stresses in the cracking analysis of Block 0 in large-span bridges. Nevertheless, it did not consider early-age autogenous shrinkage, still resulting in a certain degree of discrepancy from actual field conditions.

As evident from the above, previous studies addressing the early-age cracking of concrete structures have not comprehensively considered the early-age thermo-hygro-mechanical coupling effects [85]. The conventional approach has been to analyze thermal stresses in isolation, often ignoring early-age concrete creep effects [86], which leads to disparities between theoretical analyses and actual phenomena. With the widespread application of high-performance concrete, the early-age autogenous shrinkage effect has become increasingly prominent. Therefore, in the research on early-age cracking of large-scale precast box girders, it is imperative to comprehensively incorporate the coupling effects of early-age hydration heat, drying shrinkage, autogenous shrinkage, and creep. Only in this way can precise calculation of early-age stresses and accurate causal analysis of early-age cracks be achieved, thereby providing targeted and efficient mitigation strategies for early-age cracking in actual engineering practice [87]. The flowchart of the hygro-thermo-mechanical coupled calculation performed using ABAQUS is shown in Figure 4.

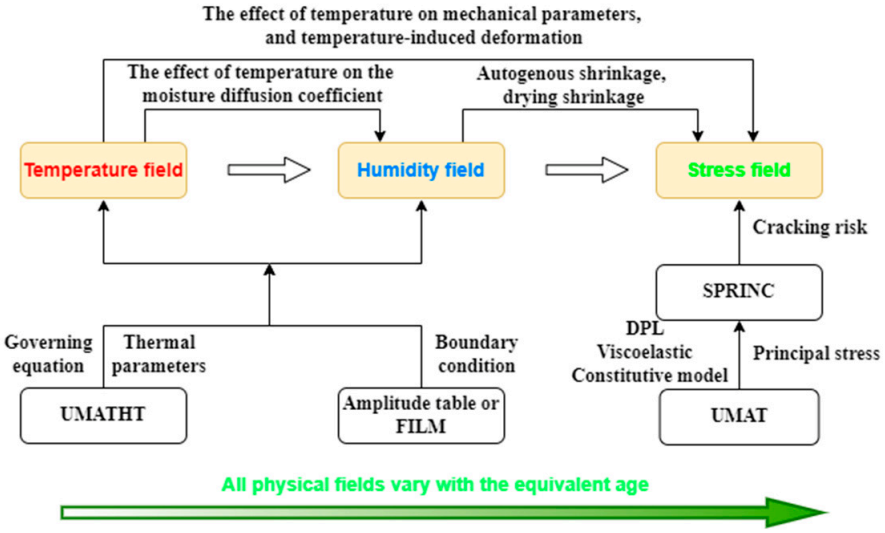


Figure 4. Flowchart of hygro-thermo-mechanical coupled calculation.

5. Control of Early-Age Cracking Risk in Large-Scale Precast Box Girders

To control early-age cracking in large-scale precast box girders and prevent the formation of early-age cracks, it is necessary to concurrently determine the control threshold for early-age concrete cracking. An excessively large control threshold may result in overly conservative construction measures that lack economic efficiency; conversely, a threshold that is too small may lead to the generation of early-age cracks.

Regarding the evaluation of concrete crack resistance, the assessment indicators vary among relevant domestic and international design codes. According to the provisions for the serviceability limit state in the Chinese Specifications for Design of Highway Reinforced Concrete and Prestressed Concrete Bridges and Culverts (JTG 3362-2018) [52], for fully prestressed concrete flexural members, the principal tensile stress σ_{tp} in the diagonal section should be less than 0.6 times the standard value of concrete tensile strength f_{tk}, as shown in Equation (4).

$$\sigma_{tp} \leq 0.6 f_{tk} \tag{4}$$

In the Chinese Design Specification for Concrete Gravity Dams (SL 319-2018) [88], a safety factor is adopted as the basis for thermal crack control. The calculation formula is defined as the ultimate tensile strain of concrete multiplied by its elastic modulus, divided by the sum of thermal stresses generated by various temperature differences; the safety factor should be controlled between 1.5 and 2.0. Additionally, the Standard for Construction of Mass Concrete (GB 50496-2018) [89] introduces a crack prevention safety factor (the ratio of the standard value of concrete tensile strength to the restrained tensile stress) as the criterion for thermal crack control, requiring this factor to be no less than 1.15 [90]. Meanwhile, the Technical Specification for Thermal Cracking Control of Mass Concrete of Port and Waterway Engineering (JTS 202-1-2022) [91] employs a temperature control cracking safety factor (the ratio of splitting tensile strength to tensile stress) as the basis for crack control, stipulating a minimum safety factor of 1.4.

In contrast, Japanese codes require that the ratio of splitting tensile strength to the calculated thermal stress must be between 1.25 and 1.5. In Europe, the concept of cracking risk is generally adopted, which is defined as the ratio of the calculated concrete tensile stress to the splitting tensile strength at the corresponding age. For instance, the Oresund Tunnel and the Great Belt Bridge in Denmark mandated that the ratio of calculated thermal stress to splitting tensile strength should not exceed 0.7 [90]. Field monitoring results

indicated that no thermal cracks occurred under this requirement, demonstrating excellent temperature control effectiveness.

Based on the above analysis, existing engineering codes typically utilize the splitting tensile strength as the computational basis for crack control. In scenarios where strict crack control is required to ensure a probability of non-cracking above 95%, the ratio of splitting tensile strength to calculated thermal stress is generally required to exceed 1.5. Studies have found that the axial tensile strength of concrete is usually lower than its splitting tensile strength, with the ratio between the two ranging from 0.8 to 1.0. Furthermore, in Chinese engineering projects, cubic specimens are conventionally used to test splitting tensile strength, which further increases the uncertainty in the relationship between these two types of tensile strength. Given these considerations, it is proposed to use the tensile strength for calculations and introduce the concept of a cracking risk coefficient to evaluate the likelihood of shrinkage cracks in concrete. Based on a literature review and statistical analysis of extensive engineering calculations and monitoring results [92], setting the control threshold for the early-age concrete cracking risk coefficient at 0.70 can balance economic efficiency with effective engineering crack prevention.

In the numerical calculation of early-age cracking risk for large-scale precast box girders, the cracking risk coefficient is expressed as the ratio of the maximum tensile stress to the time-dependent tensile strength, with 0.70 adopted as the control threshold [90], as shown in Equation (5). In Equation (5), $\sigma(t)$ represents the maximum principal tensile stress at the integration points of the finite element of concrete at time t. $f_t(t)$ represents the direct tensile strength of concrete at time t.

$$\eta = \frac{\sigma(t)}{f_t(t)} \tag{5}$$

(1) When $\eta > 1.0$, it indicates that the concrete has already cracked;
(2) When $\eta = 1.0$, it indicates that the concrete is in a critical state of cracking;
(3) When $0.7 < \eta < 1.0$, it indicates that there is a possibility of concrete cracking;
(4) When $\eta < 0.7$, it indicates that the concrete is unlikely to crack.

From the perspective of engineering cracking, shrinkage measured before the "zero point" (the point when the structure begins to form) has no mechanical significance; therefore, the final setting time of the concrete can be defined as the zero point of shrinkage. The cracking risk assessment procedure for large precast box girders at early age is shown in Figure 5. The stress field should incorporate the effects of time-dependent elastic properties and creep-induced stress redistribution. Mesh convergence should also be checked to ensure that the calculated local stress concentrations are not numerical artifacts. The cracking risk coefficient provides an engineering screening criterion for identifying potential cracking locations. Detailed simulation of crack initiation and propagation requires additional fracture-based approaches, such as damage mechanics, cohesive models, or extended finite element methods.

To prevent early-age cracking in large precast box girders, researchers have investigated the concrete placement temperature, mix design, formwork insulation, internal curing, and prestressing timing. Replacing part of the cement with fly ash and slag not only reduces the heat of hydration but also cuts carbon emissions, offering significant environmental benefits [93,94].

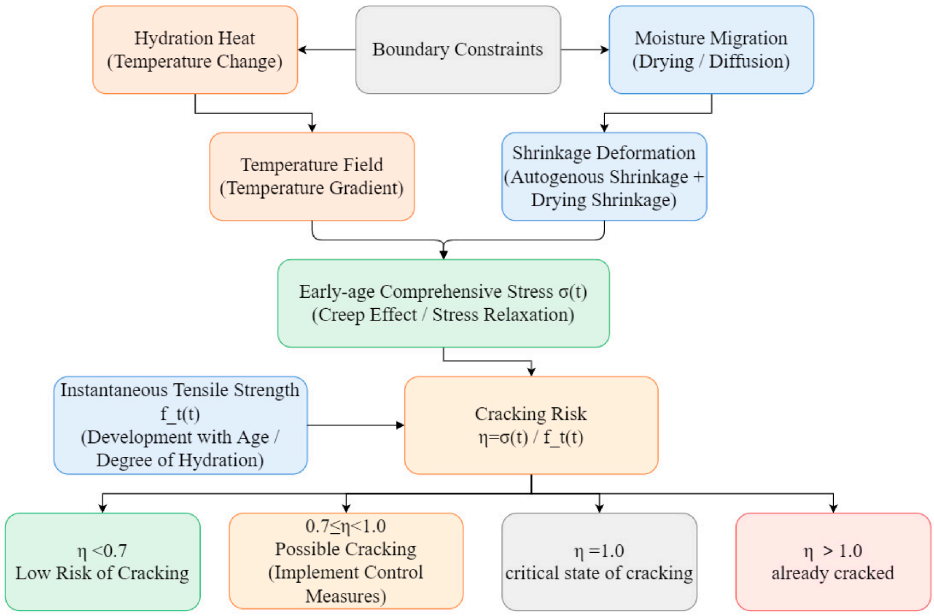


Figure 5. Cracking Risk Assessment Procedure for Large Precast Box Girders at Early Age.

6. Application of Machine Learning in Early-Age Response Studies of Large Precast Box Girders

6.1. Data-Driven Prediction of Early-Age Temperature and Humidity Fields

Early studies on the prediction of concrete hydration heat and early-age temperature fields primarily employed empirical or semi-empirical models for regression fitting of experimental data. For instance, Long et al. [95] investigated sustained sub-zero temperature environments and adopted five hydration heat models—exponential, power exponential, composite exponential, hyperbolic, and logarithmic functions—to fit and analyze errors in cement hydration heat test data. They established a prediction model for casting temperature versus hydration heat, with results indicating that the hyperbolic function model could satisfactorily predict the evolution of cement hydration heat with age under negative temperature conditions.

With the accumulation of monitoring data, machine learning methods represented by artificial neural networks (ANNs) have been gradually introduced into temperature prediction for mass concrete. Guo et al. [96] combined COMSOL finite element simulation with back-propagation (BP) neural networks, incorporating genetic algorithms and Bayesian updating to optimize network weights. This approach effectively overcame errors arising from artificially set convective heat transfer coefficients in finite element simulations and empirical assumptions in hydration heat formulas. The neural network prediction curves showed good agreement with measured temperature variations, with a maximum error of only 2.57%. Xiao [97] investigated mass concrete for the arch springing of a long-span concrete-filled steel tubular arch bridge in a mountainous area of southwestern China, establishing two types of hydration heat temperature prediction models: a static BP model and a dynamic ELMAN model. Results showed that the BP model could control static prediction accuracy for specific ages within 1 °C, while the ELMAN model, though slightly lower in single-point accuracy, could simulate and predict the entire temperature variation process curve with trends matching measured data well, achieving accuracy within 2 °C. The combined use of both models can provide effective guidance for on-site temperature control.

Data-driven methods have also been extended to humidity field and shrinkage prediction, as well as mix proportion optimization design. Sun et al. [98] systematically compared seven machine learning algorithms—including decision trees, random forests, extreme

gradient boosting, gradient boosting machines, light gradient boosting machines, and fully connected neural networks—for predicting the cumulative hydration heat and internal relative humidity of concrete. They revealed the dominant roles of key factors, such as the water-to-binder ratio and binder composition, and further combined the NSGA-II algorithm to construct a multi-objective optimization design framework for concrete mix proportions targeting low autogenous shrinkage. The above studies indicate that data-driven methods can not only substitute for some early-age performance tests that are costly and time-consuming but also bridge performance prediction with material design, providing new insights for source control of early-age cracking in large precast box girders. However, the prediction accuracy of purely data-driven models is highly dependent on the quantity and coverage of training samples, with limited extrapolation capability under out-of-sample working conditions. Moreover, the model decision-making process lacks explicit physical interpretability, which constrains its in-depth application in engineering safety-critical scenarios.

6.2. Physics-Informed Neural Networks and Thermal Parameter Inversion

The time-varying characteristics and temperature dependency of thermal parameters for large precast box girders at early age are key factors constraining accurate simulation of temperature fields, while parameter inversion represents an important approach for obtaining true thermal parameters. Traditional inverse analysis methods typically rely on long-term test data and require repeated invocation of forward models, suffering from low efficiency and high costs [99]. Zhang et al. [100] proposed an inverse analysis method for thermal parameters of mass concrete based on uniform design theory and BP neural networks. They employed uniform design to determine training samples, established a nonlinear mapping between temperature fields and thermal parameters through BP neural networks, and optimized network training using an additional momentum method. This method was successfully applied to the construction of mass concrete for the saddle pedestal cap of the Taihong Yangtze River Bridge, inverting the adiabatic temperature rise, reaction rate constant, and thermal conductivity. The temperature calculations based on inverted parameters showed good agreement with field measurements, with a maximum error of only 1.1 °C at the temperature peak.

In recent years, the emerging Physics-Informed Neural Networks (PINNs) have provided a more systematic technical framework for parameter inversion and field reconstruction. The core concept is to explicitly or implicitly embed prior knowledge such as physical governing equations and boundary conditions into deep neural networks, guiding the model to satisfy physical consistency while learning from data, thereby enhancing the model's generalization performance and credibility [101]. Bu et al. [99] applied the PINN framework to parameter inversion of the concrete hydration heat source function. By computing the residual of the heat conduction governing equation through automatic differentiation and embedding it into the loss function, they could simultaneously identify hydration heat parameters and reconstruct temperature fields using only limited temperature observation data, significantly reducing reliance on long-term intensive monitoring tests. Lee and Lee [102] further developed a PINN inverse problem modeling method for mass concrete, which could characterize cement hydration heat behavior and predict internal structural temperature distributions using only measured temperature data. Comparisons with numerical simulations based on representative empirical heat release models verified its effectiveness in thermal behavior characterization and temperature field prediction. Addressing the noise and uncertainty prevalent in engineering monitoring data, Yang et al. [103] proposed Bayesian Physics-Informed Neural Networks (B-PINNs), combining Bayesian inference with PINNs to solve forward and inverse problems of partial differential

equations under noisy data conditions and quantify prediction uncertainties, providing a theoretical tool for reliability assessment of early-age cracking risk. Notably, the modeling quality of physics-informed machine learning depends on the completeness of the embedded physical models. For example, the theoretical model for Portland cement hydration established by Liu [104], which accounts for multi-physics, multi-scale, and multi-driving-force effects, mechanistically characterizes the coupling relationships between hydration reactions and field variables such as temperature and humidity. This can provide governing equations and mechanistic constraints for constructing physics-informed models targeting early-age concrete.

7. Conclusions

Research on early-age multi-field coupling behavior in large-scale precast box girders is of great significance to the durability, safety, and service performance of bridge structures. This paper presents a systematic review focusing on the current research status of early-age temperature, moisture, stress fields, and artificial intelligence-based prediction and regulation in large-scale precast box girders. It summarizes and analyzes the formation mechanisms of early-age stresses under multi-field coupling effects and cracking risk evaluation methods, while outlining future research directions. The primary conclusions are drawn as follows:

(1) Existing studies on the early-age temperature fields of large-scale precast box girders still inadequately consider the temperature-dependent variations in hydration reaction rates and the time-varying characteristics of thermal parameters. Due to the universal use of high-performance concrete in these girders, which are characterized by a concentrated release of hydration heat, high internal temperature rise, and significant temperature gradients, the fluctuations of temperature further influence both the hydration reaction rate and the evolution of the material's thermal parameters. In current research, parameters such as thermal conductivity and specific heat capacity are frequently simplified as constants, which fails to accurately reflect the evolutionary patterns of the early-age temperature field. Therefore, future research must establish temperature field analysis models that simultaneously account for spatio-temporal effects, temperature dependencies, and the dynamic variations in thermal parameters. This will improve the prediction accuracy of early-age temperature fields and provide a reliable foundation for thermal stress analysis and the optimization of temperature control measures.

(2) Research on the evolutionary patterns of early-age moisture fields and the formation mechanisms of moisture-induced stresses in large-scale precast box girders remains relatively weak. Most existing studies merely consider the effects of drying shrinkage, neglecting the pronounced early-age autogenous shrinkage effect inherent to high-performance concrete under low water–binder ratio conditions. The combined action of autogenous shrinkage and drying shrinkage exacerbates internal moisture gradients and deformation incompatibility within the structure, thereby significantly affecting early-age stress distribution and crack development. Currently, systematic studies on the early-age moisture fields and moisture-induced stresses of these girders are scarce, and a comprehensive theoretical analysis system has yet to be established. Therefore, future efforts should strengthen the research on early-age moisture fields and moisture-induced stresses by developing analysis methods that concurrently consider both autogenous and drying shrinkage, thus further revealing the impact mechanisms of moisture-induced stresses on early-age cracking behavior.

(3) Research on the early-age stress fields of large-scale precast box girders has not yet fully achieved a synergistic analysis among the temperature, moisture, and mechanical

fields, and the consideration of early-age creep effects is insufficient. Most current studies focus primarily on thermal stress analysis. Although some studies have established thermo-mechanical coupling models, consideration of the complex coupling effects between thermal and hygral deformations remains limited. Because large-scale precast box girders exhibit evident time-dependent material properties at early ages, creep can induce stress redistribution and stress relaxation; moreover, the synergistic action of temperature and moisture is a vital trigger for early-age cracking. Therefore, future studies should construct a more comprehensive Thermo-Hygro-Mechanical (THM) multi-field coupling analysis system. By comprehensively integrating the impacts of hydration heat, autogenous shrinkage, drying shrinkage, and creep on early-age stress evolution, accurate assessment of early-age cracking risks can be achieved, thereby providing theoretical support for crack prevention and control as well as the optimization of construction technologies.

(4) Machine learning methods offer a new paradigm for overcoming the modeling bottlenecks in early-age multi-field coupled analysis of large precast box girders. Data-driven models enable efficient prediction of early-age temperature and humidity fields, whereas Physics-Informed Neural Networks (PINNs) can accomplish thermal parameter inversion and field reconstruction from sparse and noisy monitoring data. Future research should focus on addressing critical challenges, including the scarcity of field measurement data, insufficient physical consistency and interpretability of models, and limited capabilities in uncertainty quantification. It is imperative to establish an intelligent analysis framework for early-age multi-field coupling that integrates physics-based constraints with data-driven approaches, thereby achieving accurate assessment and intelligent prevention and control of cracking risk in large precast box girders.

Author Contributions: Conceptualization, Y.C.; methodology, Y.C.; investigation, M.Z.; resources, H.Z.; writing—original draft preparation, M.Z. and Y.C.; writing—review and editing, X.T.; visualization, M.Z.; supervision, X.T.; project administration, H.Z.; funding acquisition, Y.C. All authors have read and agreed to the published version of the manuscript.

Funding: This study was supported by the Ningbo Key Scientific and Technological Support Project in the Field of Transportation (Grant No. 2024032), and the Initial Scientific Research Fund of Ningbo University of Technology (Grant No. 24KQ101).

Data Availability Statement: No new data were created or analyzed in this study. Data sharing is not applicable to this article.

Conflicts of Interest: The authors declare no conflicts of interest.

References

1. Editorial Department of China Journal of Highway and Transport. Review on China's Bridge Engineering Research: 2021. *China J. Highw. Transp.* **2021**, *34*, 1–97.
2. Lu, Z. Key technologies for Hangzhou Bay Bridge. *China Civ. Eng. J.* **2006**, *6*, 78–82+87.
3. Wei, C.; Wang, C.; Ning, W. Thermo-hydro-mechanical coupling analysis of early-age concrete withbehavioral changes considered and its application. *China Civ. Eng. J.* **2015**, *48*, 44–53.
4. Wu, J.; Chen, W.; Huang, Y. Computational modeling of shrinkage induced cracking in early-age concrete based on theunified phase-field theory. *Chin. J. Theor. Appl. Mech.* **2021**, *53*, 1367–1382.
5. Li, X.; Liu, W.; Ren, J.; Yang, R.; Liu, X. Time Varying Behavior of Early-age Concrete of Double-block Ballastless Track Based on Multi-physical Field Coupling. *J. China Railw. Soc.* **2023**, *45*, 91–102.
6. Wang, J.; Lv, Z.; Zhao, Z.; Liu, C.; Sun, Y. Control of the Early Cracks in the Top Slab of the Prestressed Concrete Continuous BoxGirder. *J. Railw. Eng. Soc.* **2019**, *36*, 43–48.
7. Zhang, P.; Xiong, H.; Wang, R. Measurements and numerical simulations for cast temperature field and early-age thermal stress in zero blocks of high-strength concrete box girders. *Adv. Mech. Eng.* **2022**, *14*, 168781322210915. [CrossRef]

8. Sheng, X.; Xiao, S.; Zheng, W.; Sun, H.; Yang, Y.; Ma, K. Experimental and finite element investigations on hydration heat and early cracks in massive concrete piers. *Case Stud. Constr. Mater.* **2023**, *18*, e01926. [CrossRef]
9. Wang, J.; Fang, Z.; Liu, J.; Zuo, Y.; Ma, Z. Research on the Construction Crack Resistance of Large-span Box Girder Bridge. *J. Railw. Eng. Soc.* **2016**, *33*, 81–86.
10. Schackow, A.; Effting, C.; Gomes, I.R.; Patruni, I.Z.; Vicenzi, F.; Kramel, C. Temperature variation in concrete samples due to cement hydration. *Appl. Therm. Eng.* **2016**, *103*, 1362–1369. [CrossRef]
11. Luo, J. Experimental Study on the Time-Dependent Effects of Shrinkage, Creep and Temperature on PC Box Girder Bridge in High-Speed Railway. Ph.D. thesis, Central South University, Changsha, China, 2014.
12. Wei, D.; Du, C.; Lin, Y.; Chang, B. Impact factors of hydration heat of cemented tailings backfill based on multi-index optimization. *Case Stud. Therm. Eng.* **2020**, *18*, 100601. [CrossRef]
13. Do, T.A.; Verdugo, D.; Tia, M.; Hoang, T.T. Effect of volume-to-surface area ratio and heat of hydration on early-age thermal behavior of precast concrete segmental box girders. *Case Stud. Therm. Eng.* **2021**, *28*, 101448. [CrossRef]
14. Zhang, N.; Zhou, X.; Liu, Y.; Liu, J. N-situ test on hydration heat temperature of box girder based on array measurement. *China Civ. Eng. J.* **2019**, *52*, 76–86.
15. Chang, S.; Yang, M.; Sun, Y.; Liu, K. Calculation Method of Early-Age Crack Width in Reinforced Concrete Bridge through a Nonlinear FEA Model. *KSCE J. Civ. Eng.* **2019**, *23*, 3088–3096. [CrossRef]
16. Liu, Y.; Liu, J. Review on temperature action and effect ofsteel-concrete composite girder bridge. *J. Traffic Transp. Eng.* **2020**, *20*, 42–59.
17. Chen, B.; Ding, R.; Zheng, J.; Zhang, S. Field test on temperature field and thermal stress for prestressed concrete box-girder bridge. *Front. Archit. Civ. Eng. China* **2009**, *3*, 158–164. [CrossRef]
18. Wu, H.; Liu, J. Investigations of the Temperature Field and Cracking Risk in Early Age Massive Concrete in the # 0 Segment of a Box Girder Bridge. *KSCE J. Civ. Eng.* **2023**, *27*, 3971–3989. [CrossRef]
19. Hui, Y.; Sun, X.; Wang, H.; Zhang, Y. Study on Temperature Effect of Long-span Variable Cross-sectionConcrete Box Girder during Construction. *J. Highw. Transp. Res. Dev.* **2023**, *40*, 98–105.
20. Yu, Y.; Zhang, F.; Zhang, L.; Liu, J. Test and analysis on hydration of concrete three-cell box girder. *J. Southeast Univ. (Nat. Sci. Ed.)* **2022**, *52*, 1043–1051.
21. Wang, P.; Huang, C.; Zhao, G.; Zhang, F. Experiment of the model of hydration heat temperature field and strain field of concrete single box and three chamber girder. *J. Shandong Univ. (Eng. Sci.)* **2024**, *54*, 109–122.
22. Wang, J.; Fang, Z.; Liu, J. Measurement and Analysis of HydrationHeat of Long Span PC Box Girders. *Bridge Constr.* **2016**, *46*, 29–34.
23. Zhang, Z.; Liu, Y.; Liu, J.; Zhang, N. Thermo-mechanical behavior simulation and cracking risk evaluation on steel-concrete composite girders during hydration process. *Structures* **2021**, *33*, 3912–3928. [CrossRef]
24. Han, S.; Liu, Y.; Lyu, Y.; Liu, J.; Zhang, N. Numerical simulation investigation on hydration heat temperature and early cracking risk of concrete box girder in cold regions. *J. Traffic Transp. Eng. (Engl. Ed.)* **2023**, *10*, 697–720. [CrossRef]
25. Knor, G.; Jaskulski, R.; Glinicki, M.A.; Holnicki-Szulc, J. Numerical identification of the thermal properties of early age concrete using inverse heat transfer problem. *Heat Mass Transf.* **2019**, *55*, 1215–1227. [CrossRef]
26. Cui, W.; Luo, Y.; Peng, S. Early-Age Cracking Analysis of a HVFA Concrete Structure Based on Thermo-Hygro-Mechanical Modeling Combined with XFEM. *Adv. Mater. Sci. Eng.* **2020**, *2020*, e5793902. [CrossRef]
27. Chen, B.; Guan, B.; Lu, X.; Tian, B.; Li, Y. Thermal conductivity evolution of early-age concrete under variable curing temperature: Effect mechanism and prediction model. *Constr. Build. Mater.* **2022**, *319*, 126078. [CrossRef]
28. De Schutter, G. Finite element simulation of thermal cracking in massive hardening concrete elements using degree of hydration based material laws. *Comput. Struct.* **2002**, *80*, 2035–2042. [CrossRef]
29. Xu, P.; Zhu, Y.; Ben, N. Model of Adiabatic Temperature Rise of Concrete and Its Application. *J. Basic Sci. Eng.* **2011**, *19*, 243–250.
30. Cai, Y.; Wang, F.; Zhao, Z.; Lyu, Z.; Wang, Y.; Zou, P. Early-Hydration heat and influencing factor analysis of Large-Volume concrete box girder based on equivalent age. *Structures* **2023**, *50*, 1699–1713. [CrossRef]
31. Zeng, Y.; Zeng, Y.; Jiang, D.; Liu, S.; Tan, H.; Zhou, J. Curing parameters' influences of early-age temperature field in concrete continuous rigid frame bridge. *J. Clean. Prod.* **2021**, *313*, 127571. [CrossRef]
32. Wang, X.; Wang, W.; Huang, J.; Wang, Z.; Ma, S.; Liu, Y. Relationship between internal humidity and drying shrinkage of recycled aggregate thermal insulation concrete considering recycled aggregate content. *Constr. Build. Mater.* **2022**, *355*, 129224. [CrossRef]
33. Chen, X.; Zhang, H.; Geng, Y.; Wang, Y.-Y. Tests and prediction model for time-dependent internal relative humidity of recycled aggregate concrete due to self-desiccation. *Constr. Build. Mater.* **2022**, *352*, 129024. [CrossRef]
34. Zhu, J.; Wang, C.; Yang, Y.; Wang, Y. Hygro-thermal–mechanical coupling analysis for early shrinkage of cast in situ concrete slabs of composite beams: Theory and experiment. *Constr. Build. Mater.* **2023**, *372*, 130774. [CrossRef]
35. Zhang, J.; Qi, K.; Huang, Y. Calculation of Moisture Distribution in Early-Age Concrete. *J. Eng. Mech.* **2009**, *135*, 871–880. [CrossRef]

36. Liu, J.; Tian, Q.; Wang, Y.; Li, H.; Xu, W. Evaluation Method and Mitigation Strategies for Shrinkage Cracking of Modern Concrete. *Engineering* **2021**, *7*, 168–188. [CrossRef]
37. Tazawa, E.I.; Miyazawa, S. Experimental study on mechanism of autogenous shrinkage of concrete. *Cem. Concr. Res.* **1995**, *25*, 1633–1638. [CrossRef]
38. Chao, P.; Zheng, J.; Wang, X. Numerical algorithm for moisture diffusion in highperformance concrete. *J. Fuzhou Univ. (Nat. Sci.)* **2007**, *06*, 898–903.
39. Xi, Y.; Bažant, Z.P.; Jennings, H.M. Moisture diffusion in cementitious materials Adsorption isotherms. *Adv. Cem. Based Mater.* **1994**, *1*, 248–257. [CrossRef]
40. Yuan, Y.; Wan, Z.L. Prediction of cracking within early-age concrete due to thermal, drying and creep behavior. *Cem. Concr. Res.* **2002**, *32*, 1053–1059. [CrossRef]
41. Wang, J. Studies on Humidity Field and Shrinkage Stress of Ordinary AndInternally Cured Concrete. Ph.D. thesis, Tsinghua University, Beijing, China, 2018.
42. Maruyama, I.; Lura, P. Properties of early-age concrete relevant to cracking in massive concrete. *Cem. Concr. Res.* **2019**, *123*, 105770. [CrossRef]
43. Chen, Z.; Cui, J.; Zhu, J.; An, M.; Yu, Z. Analysis and control of cracking in reinforced concrete. *Eng. Mech.* **2006**, *S1*, 86–107.
44. Zhu, Y.; Zhan, S. Study on Reasons and Prevention Measures ofCracking in Concrete Structure. *J. Mater. Sci. Eng.* **2003**, *5*, 727–730.
45. Wang, N. Multi-Field Coupling Analysis of Early-AgeConcrete and Its Application Considering Changing of Behavior. Master's thesis, Tianjin University, Tianjin, China, 2014.
46. Li, Y.; Tan, M.; Zhang, X.; Wu, K. Autogenous Shrinkage of Concrete and Its Research Progress. *J. Build.* **2000**, *3*, 252–257.
47. Ma, Y. Study on Temperature and Stress of Concrete Based on Degree of Hydration. Ph.D. thesis, Hohai University, Nanjing, China, 2006.
48. Zhu, Y. Experimental Investigation and Theoretical Modeling on Early-Age Shrinkage Cracking in Concrete. Master's thesis, Zhejiang University, Hangzhou, China, 2005.
49. Hou, D. Integrative Studies on Autogenous and Drying Shrinkage of Concreteand Related Issues. Ph.D. thesis, Tsinghua University, Beijing, China, 2010.
50. Zhu, Y.; Liu, Y.; Cao, W.; Wu, J. Analysis of concrete moisture dry shrinkage and stress based on mesoscopical model. *Shuili Xuebao* **2006**, *10*, 1163–1168.
51. He, J.; He, T.; Yang, C.; Wang, Z. Influence of Carbonation on Drying Shrinkage of Alkali-Activated Slag Cement Stone. *J. Build. Mater.* **2015**, *18*, 221–227.
52. *JTG 3362-2018*; Specifications for Design of Highway Reinforced Concrete and Prestressed Concrete Bridges and Culverts. CCCC Highway Consultants Co., Ltd.: Beijing, China, 2018.
53. Peng, Q. Research on Control of Shrinkage Cracksin Super-Long Concrete Structure. Ph.D. thesis, Tianjin University, Tianjin, China, 2012.
54. Li, S. Study on Time-Depending Structural Behavior of Long-Span Cantilever Casting Pc Box Girder Bridges Based on Thermo-hydro-mechanical Combined Effects Analysis. Ph.D. thesis, Southwest Jiaotong University, Chengdu, China, 2019.
55. Wang, T. Cracking Control of Reinforced Concrete Construction. *Concrete* **2000**, *5*, 3–6.
56. Wang, J.; Lv, P.; Xu, Q.; Luo, X.; Zhu, M. Calculation model for concrete creep and its practical application. *Eng. Mech.* **2018**, *35*, 156–160.
57. *GB 50010-2010*; Code for Design of Concrete Structures. Ministry of Housing and Urban-Rural Development of the People's Republic of China: Beijing, China, 2010.
58. Springenschmid, R. *Prevention of Thermal Cracking in Concrete at Early Ages*; China Building Materials Press: Beijing, China, 2019.
59. Hu, C.; Sun, Z.; Wang, L. Early-age Creep Effects of Cement Concrete Pavement. *Eng. Mech.* **2022**, *39*, 123–137.
60. Otto, R.R. Development of an Early-Age Behavior Model for Portland Cement Concrete Pavements. Ph.D. thesis, The University of Texas at Austin, Austin, TX, USA, 1996.
61. Zhang, J.; Qi, K.; Zhang, M. Calculation of the Thermal Stresses in Concrete Pavements at Early Ages. *Eng. Mech.* **2007**, *11*, 136–145.
62. Zhang, J.; Hou, D.; Gao, Y. Calculation of Shrinkage Stress in Early-Age Concrete Pavements. II: Calculation of Shrinkage Stress. *J. Transp. Eng.* **2013**, *130*, 971–980. [CrossRef]
63. Liang, S.; Wei, Y. Modelling of creep effect on moisture warping and stress developments in concrete pavement slabs. *Int. J. Pavement Eng.* **2018**, *19*, 429–438. [CrossRef]
64. Wang, L.; Hu, C.; Zeng, Y. Numerical Analysis of Early-age Curling Behavior of Cement Concrete Pavement. *Eng. Mech.* **2017**, *34*, 146–155.
65. Zhang, C. Study on Thermodynamic Evolution of Concrete with Chemo-Thermo-Mechanical Couplings and Temperature Control and Cracking Prevention Method. Ph.D. thesis, Wuhan University, Wuhan, China, 2015.
66. Tao, Z.; Weizu, Q. Creep of Concrete at Early Age and its Effecton Cracking Sensitivity. *Ind. Constr.* **2005**, *8*, 89–92+105.

67. De Schutter, G. Applicability of degree of hydration concept and maturity method for thermo-visco-elastic behaviour of early age concrete. *Cem. Concr. Compos.* **2004**, *26*, 437–443. [CrossRef]
68. Neville, A.M.; Dilger, W.H.; Brooks, J.J. *Creep of Plain and Structural Concrete*; Construction Press: London, UK; New York, NY, USA, 1983.
69. Bažant, Z.P. Thermodynamics of Solidifying or Melting Viscoelastic Material. *J. Eng. Mech. Div.* **1979**, *105*, 933–952. [CrossRef]
70. Bažant, Z.P.; Prasannan, S. Solidification Theory for Concrete Creep. II: Verification and Application. *J. Eng. Mech.* **1989**, *115*, 1704–1725. [CrossRef]
71. Bažant, Z.P.; Hauggaard, A.B.; Baweja, S.; Ulm, F.-J. Microprestress-Solidification Theory for Concrete Creep. I: Aging and Drying Effects. *J. Eng. Mech.* **1997**, *123*, 1188–1194. [CrossRef]
72. Bažant, Z.P.; Cusatis, G.; Cedolin, L. Temperature Effect on Concrete Creep Modeled by Microprestress-Solidification Theory. *J. Eng. Mech.* **2004**, *130*, 691–699. [CrossRef]
73. Wang, T. *Control of Cracking in Engineering Structure (Second Edition)*; China Architecture & Building Press: Beijing, China, 2017.
74. Bazant, Z.P. *Mathematical Modeling of Creep and Shrinkage of Concrete*; John Wiley and Sons: Hoboken, NJ, USA, 1988.
75. de Borst, R.; van den Boogaard, A.H. Finite-Element Modeling of Deformation and Cracking in Early-Age Concrete. *J. Eng. Mech.* **1994**, *120*, 2519–2534. [CrossRef]
76. Gong, L. Research on Performance of Self-compacting Concrete and Time Dependent Multi-Field Coupling Analvsis of Concrete. Ph.D. thesis, Zhejiang University, Hangzhou, China, 2010.
77. Yu, P.; Duan, Y.; Fan, Q.; Tang, S. Improved MPS model for concrete creep under variable humidity and temperature. *Constr. Build. Mater.* **2020**, *243*, 118183. [CrossRef]
78. Liu, J.; Liu, Y.; Zhang, N.; Ma, Z.; Bai, Y. Research on temperature action and cracking risk of steel–concrete composite girder during the hydration process. *Arch. Civ. Mech. Eng.* **2020**, *20*, 47. [CrossRef]
79. Wang, F. Monitoring and Analysis of Hydration Heat Temperature and Strain of Asymmetric Prestressed Concrete Box Girder. *Railw. Eng.* **2021**, *61*, 41–43.
80. Yan, B.; Liu, W. Causes and Prevention of Early Cracks in Prestressed Concrete Box Girder. *Constr. Technol.* **2023**, *52*, 62–66.
81. Dong, L.; Hansen, C.; Wan, D. Analysis of hydration heat temperatureand strain field in the zero block. *J. Beijing Jiaotong Univ.* **2018**, *42*, 51–56.
82. Srimook, P.; Maruyama, I.; Shibuya, K.; Tomita, S.; Igarashi, G.; Hibino, Y.; Yamada, K. Evaluation of thermal crack width and crack spacing in massive reinforced concrete structures subject to external restraints using RBSM. *Eng. Fract. Mech.* **2022**, *274*, 108800. [CrossRef]
83. Qiao, G.; Xue, G.; Zhu, G. A precise internal-stress calculation algorithm for the evolution of cracking risk of the steam-curing box girder. *Constr. Build. Mater.* **2022**, *346*, 128463. [CrossRef]
84. Li, S.; Yang, Y.; Pu, Q.; Wen, W.; Yan, A. Thermo-Hydro-Mechanical Combined Effect Analysis Model for Early-Age Concrete Bridges and Its Application. *Adv. Civ. Eng.* **2020**, *2020*, e8864109. [CrossRef]
85. Wang, Y.; Zhu, J.; Guo, Y.; Wang, C. Early shrinkage experiment of concrete and the development law of its temperature and humidity field in natural environment. *J. Build. Eng.* **2023**, *63*, 105528. [CrossRef]
86. Xie, Y.; Du, W.; Xu, Y.; Peng, B.; Qian, C. Temperature field evolution of mass concrete: From hydration dynamics, finite element models to real concrete structure. *J. Build. Eng.* **2023**, *65*, 105699. [CrossRef]
87. Cai, Y.; Chen, Z.; Wang, F.; Zhao, Z.; Lyu, Z.; Wang, L.; Yan, X. Early cracking risk analysis of large precast box girders based on thermo-hygro-mechanical coupling. *Structures* **2026**, *86*, 111254. [CrossRef]
88. *SL 319-2018*; Design Specification for Concrete Gravity Dams. Changjiang Institute of Survey, Planning, Design and Research Co., Ltd.: Wuhan, China, 2018.
89. *GB 50496-2018*; Standardfor Construction of Mass Concrete. Ministry of Housing and Urban-Rural Development of the People's Republic of China: Beijing, China, 2018.
90. Liu, J. *Early Deformation and Shrinkage Crack Control of Modern Concrete*; Science Press: Beijing, China, 2020.
91. *JTS 202-1-2022*; Technical Specification for Thermal Cracking Control of Mass Concrete of Port and Waterway Engineering. CCCC Wuhan Harbour Engineering Design and Research Institute Co., Ltd.: Wuhan, China, 2022.
92. Wang, T. *Control of Cracking in Engineering Structureprinciple of "Resist and Release" Foralternative Bay Construction Method Cracking-control of Super Long Mass Concrete*; China Architecture & Building Press: Beijing, China, 2007.
93. Yoo, D.-Y.; Banthia, N.; You, I.; Lee, S.-J. Recent advances in cementless ultra-high-performance concrete using alkali-activated materials and industrial byproducts: A review. *Cem. Concr. Compos.* **2024**, *148*, 105470. [CrossRef]
94. Bolina, F.L.; Henn, A.S. Eco-Friendly Reinforced Concrete Beams Exposed to Standardized Fire: A Thermal Finite Element Analysis. *Sustainability* **2025**, *17*, 2951. [CrossRef]
95. Long, Z.; Zhang, R.; Guo, H.; Duan, Y.; Xiao, P.; Duan, Y. Influence and prediction model of molding temperature on cement hydration heat in continuous negative temperature environment. *J. Cent. South Univ. (Sci. Technol.)* **2022**, *53*, 2777−2788.

96. Guo, S.; Zhou, S. Study on temperature evolution rule and prediction method of mass concrete under natural condition. *Water Resour. Hydropower Eng.* **2018**, *49*, 188–196.
97. Xiao, Q. Research on Hydration Heat Analysis and Temperature Prediction Model for Mass Concrete Based on Multiple Boundary Conditions. Master's thesis, Chongqing Jiaotong University, Chongqing, China, 2025.
98. Sun, M.; Mao, X.; Jia, P.; Lin, Y.; Jiang, Y.; Gao, X. Machine learning-based hydration heat and relative humidity modeling for optimized design of low-autogenous shrinkage concrete. *Constr. Build. Mater.* **2025**, *504*, 144609. [CrossRef]
99. Bu, Y.; Xue, B.; Huang, Z.; Yang, M.; Zhang, Z.; Zheng, C. Parameter inversion of the concrete hydration heat source based on physics-informed neural network. *Int. J. Heat Mass Transf.* **2026**, *260*, 128409. [CrossRef]
100. Zhang, Y.; Ma, C.; Li, C.; Gao, S. Inverse analysis on thermal parameters of mass concrete based on uniform design and BP neural network. *J. Civ. Environ. Eng.* **2021**, *43*, 148–157.
101. Shan, D.; Yu, Z.; Sun, R. Bridge structural health monitoring based on physics-informed neural networks: Research advances and review. *J. Southwest Jiaotong Univ.* **2026**, *61*, 855–877.
102. Lee, J.M.; Lee, C.J. Physics-informed neural networks for inverse modeling of heat generation and temperature field in mass concrete. *Comput. Struct.* **2026**, *320*, 108035. [CrossRef]
103. Yang, L.; Meng, X.; Karniadakis, G.E. B-PINNs: Bayesian physics-informed neural networks for forward and inverse PDE problems with noisy data. *J. Comput. Phys.* **2021**, *425*, 109913. [CrossRef]
104. Liu, Y. Theoretical Model and Mechanism of Portland Cement Hydration Under Multiphysics-Multiscale-Multidrive Effect. Ph.D. thesis, Wuhan University of Technology, Wuhan, China, 2023.

Disclaimer/Publisher's Note: The statements, opinions and data contained in all publications are solely those of the individual author(s) and contributor(s) and not of MDPI and/or the editor(s). MDPI and/or the editor(s) disclaim responsibility for any injury to people or property resulting from any ideas, methods, instructions or products referred to in the content.